Physics in Medicine & Biology

IPEM Institute of Physics and Engineering in Medicine

PAPER

Spatial and polarity precision of concentric high-definition transcranial direct current stimulation (HD-tDCS)

To cite this article: Mahtab Alam *et al* 2016 *Phys. Med. Biol.* **61** 4506

IOP Publishing | Institute of Physics and Engineering in Medicine Physics in Medicine & Biology

Phys. Med. Biol. **61** (2016) 4506–4521 doi:10.1088/0031-9155/61/12/4506

Spatial and polarity precision of concentric high-definition transcranial direct current stimulation (HD-tDCS)

Mahtab Alam, Dennis Q Truong[1], Niranjan Khadka and Marom Bikson

Department of Biomedical Engineering, The City College of New York, City University of New York, New York, USA

E-mail: dtruong@ccny.cuny.edu

Received 17 November 2015, revised 13 April 2016
Accepted for publication 14 April 2016
Published 25 May 2016

Abstract

Transcranial direct current stimulation (tDCS) is a non-invasive neuromodulation technique that applies low amplitude current via electrodes placed on the scalp. Rather than directly eliciting a neuronal response, tDCS is believed to modulate excitability—enhancing or suppressing neuronal activity in regions of the brain depending on the polarity of stimulation. The specificity of tDCS to any therapeutic application derives in part from how electrode configuration determines the brain regions that are stimulated. Conventional tDCS uses two relatively large pads ($>25\,cm^2$) whereas high-definition tDCS (HD-tDCS) uses arrays of smaller electrodes to enhance brain targeting. The 4×1 concentric ring HD-tDCS (one center electrode surrounded by four returns) has been explored in application where focal targeting of cortex is desired. Here, we considered optimization of concentric ring HD-tDCS for targeting: the role of electrodes in the ring and the ring's diameter. Finite element models predicted cortical electric field generated during tDCS. High resolution MRIs were segmented into seven tissue/material masks of varying conductivities. Computer aided design (CAD) model of electrodes, gel, and sponge pads were incorporated into the segmentation. Volume meshes were generated and the Laplace equation ($\nabla \cdot (\sigma \nabla V) = 0$) was solved for cortical electric field, which was interpreted using physiological assumptions to correlate with stimulation and modulation. Cortical field intensity was predicted to increase with increasing ring diameter at the cost of focality while uni-directionality decreased. Additional surrounding ring electrodes

[1] Correspondence: Dennis Truong, Neural Engineering Laboratory, Department of Biomedical Engineering, The City College of New York, City University of New York, 85 St. Nicholas Terrace, 3366 Center for Discovery and Innovation, New York, NY 10031, Lab: 212-650-7076.

increased uni-directionality while lowering cortical field intensity and increasing focality; though, this effect saturated and more than 4 surround electrode would not be justified. Using a range of concentric HD-tDCS montages, we showed that cortical region of influence can be controlled while balancing other design factors such as intensity at the target and uni-directionality. Furthermore, the evaluated concentric HD-tDCS approaches can provide categorical improvements in targeting compared to conventional tDCS. Hypothesis driven clinical trials, based on specific target engagement, would benefit by this more precise method of stimulation that could avoid potentially confounding brain regions.

Keywords: transcranial direct current stimulation, tDCS, HD-tDCS, neuromodulation, transcranial electrical stimulation, electromagnetic modeling, medical applications

(Some figures may appear in colour only in the online journal)

1. Introduction

Transcranial direct current stimulation (tDCS) is a non-invasive neuromodulation technique that applies current through electrodes placed on the scalp (Nitsche and Paulus 2000). The applied constant current induces an electric field in the cortex (Datta *et al* 2009, Wagner *et al* 2014) which in turn modulates excitability—enhances or suppresses neuronal activity in regions of the brain (Antal *et al* 2004). The principle of excitability modulation has been used to design trials aim at a diverse range of clinical indications including depression treatment, pain control in patients with traumatic spinal cord injuries, motor rehabilitation, speech rehabilitation, and working memory (Fregni *et al* 2005, 2006, Hummel *et al* 2005, Baker *et al* 2010, Alonzo *et al* 2012). Across indications, the ability to guide current to specific brain regions is assumed to underlie efficacy and specificity and the current flow is determined by tDCS dose (defined in Peterchev *et al* 2012) along with individual anatomy (Datta *et al* 2012). Typical configuration of 'conventional' tDCS comprises current delivery from a constant direct current stimulator using a 5 × 7 cm or 5 cm × 5 cm sponge pad-covered rubber electrodes (one anode and one cathode (1 × 1)) to the desired brain target. To overcome limitations in targeting with conventional tDCS (Baker *et al* 2010), the 4 × 1 concentric ring high-definition (HD) tDCS configuration (4 × 1 HD-tDCS) has been explored as an alternative montage (Datta *et al* 2009, Suh *et al* 2009, Edwards *et al* 2013) but (Borckardt *et al* 2009, Caparelli-Daquer *et al* 2012, Brunyé *et al* 2014, Roy *et al* 2014, Heimrath *et al* 2015, Nikolin *et al* 2015, Shekhawat *et al* 2016, Zito *et al* 2015, Castillo-Saavedra *et al* 2016, Flood *et al* 2016, Kuo *et al* 2013) we note that 4 × 1 deployment is only one HD configuration and others have been implemented (Dmochowski *et al* 2013, Kempe *et al* 2014, Donnell *et al* 2015, Xu *et al* 2015).

The 4 × 1 HD-tDCS montage consists of five circular electrodes, each with radius 5.5 mm (Villamar *et al* 2013a). One electrode is placed over the target area, serving as the 'active' electrode of either anode or cathode polarity. The other four electrodes are placed in a circle at equidistance from the center (typically 5 cm) and all have the opposite polarity serving as 'returns'. One advantage of 4 × 1 HD-tDCS is that it stimulates only the part of the brain directly underneath the electrodes, since the current enters through the center electrode and is collected across the other four (Datta *et al* 2009). The rational for four electrodes in the ring

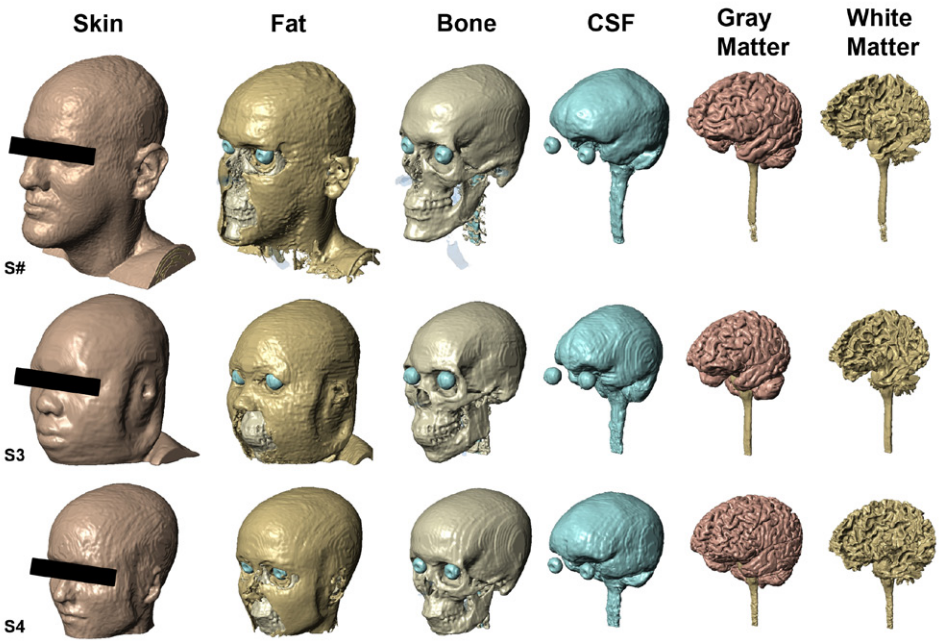

Figure 1. Segmentation masks of three individuals of varying age, weight, and gender. Seven tissues (skin, fat, skull, cerebral spinal fluid (CSF), gray matter, white matter, and air) were segmented using a combination of automated and manual techniques. Particular care was placed on maintaining continuity of thin tissues such as bone and CSF, which were the most resistive and conductive tissues, respectively. Images are on the same scale.

is to approximate a complete ring, since applying a ring electrode; especially across hair, may not reliably control current delivery (e.g. one side of ring carries more current). A radius of ~5 cm provides peak electric fields in the brain comparable to the conventional tDCS. With an increasing interest in the 4 × 1 HD-tDCS, it is worthwhile to re-consider in modeling the optimization of HD with a concentric ring montage. Some approaches to be considered are the optimal number of electrodes in the ring (if not four) and the advantages or trade-offs of the HD-tDCS as the ring radius is changed.

Computational modeling is an accepted tool for predicting current flow and tDCS dosing strategies, with ongoing validation studies (Datta *et al* 2013, Villamar *et al* 2013a, Antal *et al* 2014) and also serves as a gold-standard to determine the relationship between tDCS dose and induced brain electric fields (Minhas *et al* 2012, Edwards *et al* 2013, Miranda *et al* 2013). Here in this study we used finite element method (FEM) to predict the effects of ring radius and the number of electrodes on HD-tDCS. We created several high resolution models with various ring radii across three subjects to allow an initial consideration of inter-individual variations. In addition, models were created with different combinations of return electrodes around the center. Predicted electric field magnitude and intensity normal to the cortical surface were the primary outcomes based on the quasi-uniform assumption (Bikson *et al* 2013, 2015) and the presumed role of current direction (Bikson *et al* 2004, Rahman *et al* 2013).

2. Materials and methods

2.1. MRI information

Magnetic resonance imaging MRI scans of three human subjects who participated in a prior tDCS computational modeling study (Truong *et al* 2013) were obtained. The first subject was a 36 year-old male with a 1 mm T1-weighted MRI scan (S#), a head scan was obtained from a 22 year-old female with a 1 mm T1-weighted MRI scan (S3) and a third MRI scan was of a 25 year-old female with a 1 mm T1-weighted MRI scan (S4). Multiple MRI scans were used in this study in order to compare results and trends across individuals (figure 1).

2.2. Segmentation of MRIs into distinct tissues

Each of the MRI scans was segmented into seven tissue masks namely skin, fat, bone, CSF, gray matter, white matter, and air. First, the automatic segmentation using the algorithms from Statistical Parametric Mapping (SPM8, Wellcome Trust Centre for Neuroimaging, London, UK) was implemented. A MATLAB script was then used to smooth artifacts and correct for discontinuities (Huang *et al* 2013). Finally, a manual segmentation was performed using ScanIP ((an image processing software) Simpleware Ltd, Exeter, UK) to remove any remaining continuity or detail errors in all tissues.

2.3. Modeling HD-tDCS using FEM

The HD-tDCS electrodes and gel were modeled in SolidWorks (Dassault Systèmes Corp., Waltham, MA) as a computer aided design (CAD) file and were manually placed on the targeted area in each of the segmented head models using ScanCAD (Simpleware Ltd, Exeter, UK). In order to investigate the effect of ring radius on peak electric field, the electrodes were placed in the 4×1 HD-tDCS montage, centered over the motor strip (C3 in the 10–20 system). This was the only type of electrode configuration modeled; however, five different ring radii were modeled for each of the three subjects, for a total of fifteen models. The anodal disk electrode (11 mm diameter) was placed on top of a layer of gel and was positioned over the primary motor cortex, corresponding to C3. Four identical cathodal electrodes were positioned in a circle, each at the same fixed distance (5 cm) from the anode. As previously described, the center anode was placed over C3 and eight models were solved on head S#, with the number of cathodes in each increasing from one to eight. While on head S3 and S4, five cathode combinations with one center anode were solved—one, three, four, five, and seven cathodes.

A volumetric mesh was generated with an elements size of 6×10^6 to 14×10^6 using COMSOL Multiphysics (COMSOL Inc., Burlington, MA). The following electrical conductivities (S/m) from a previous study were assigned to each of the tissues and electrodes: Skin 0.465, Fat 0.025, Bone 0.01, CSF 1.65, Gray matter 0.276, White matter 0.126, Air 1×10^{15}, Electrodes 5.99×10^7, and Gel 0.3 (Wagner *et al* 2007). Laplace equation ($\nabla \cdot (\sigma \nabla V) = 0$) ($V$: potential, σ: conductivity) was solved with the following boundary conditions: the exposed surface of the anode was assigned a normal current density of $1\ \mathrm{A\ m^{-2}}$ ($-n \cdot J = 1$), the exposed surface of the cathode were grounded ($V = 0$), internal boundaries were assigned continuity ($n \cdot (J_1 - J_2) = 0$), and the rest of the surfaces were considered insulated ($n \cdot J = 0$). Electric field magnitude and cross-sectional slice plots of the cortical surface were generated for each model to investigate the modulation of neuronal excitability as a function of applied electric fields (Bikson *et al* 2004, 2013, 2015).

3. Results

3.1. Segmentation and normalization

We adapted previously developed head models (Datta *et al* 2012, Truong *et al* 2013). Our workflow preserved the resolution of the initial MRI scans (1 mm) while further enhancing precision by incorporating appropriate information on the tissue anatomy including the continuity of CSF (e.g. brain does not contact skull). Unless otherwise indicated, we predicted brain electric fields for a center current of 1 mA; acknowledging that electric field scales linearly with current, hence results can be represented as electric field per applied current and relative differences across simulations would remain robust. Likewise, current flow is linear (symmetric) with the montage so we simulated only the case with a center anode and surrounding cathodes, but results for cathode center simply invert the electric field direction and relative differences across simulations would be robust as well.

3.2. General role of ring radius

We predicted brain electric field for the 4×1 HD-tDCS by varying ring radius and the distance between the center electrode and ring electrodes (fifteen models, five different radii per three head; figure 2(A)). Electric field intensity increased with the ring radius (as the surround electrodes are moved further away from the center electrode). In all cases, the electric field was peak underneath the center electrode and the brain current distribution is largely restricted to the cortical area circumscribed by the ring electrode. This general finding was robust across subjects (S#, S3, S4) though there were variations in peak electric field reflecting gross anatomical differences (e.g. skull thickness) and detailed of current flow reflecting idiosyncratic anatomical differences (e.g. cortical folding). Thus, outside these cortical areas defined by the ring, there was minimal current hence minimal electric field. Relative depth of current penetration was increased with increasing the ring radius (figure 2(B)). Note that the lower conductivity of white matter produces an apparent increase in electric field in deeper regions, though current density continues to drop. Electric field is proportional to current density divided by conductivity, ($E = J/\sigma$). Sudden changes in tissue conductivity can lead to discontinuous scaling of the otherwise continuous current density, which in turn leads to the electric field peaks at the white matter/grey matter boundary. However, the influence of subthreshold electric fields and current density on white matter (axon tracts) has less mechanistic support than cortical electric field (Bikson *et al* 2004, Rahman *et al* 2013).

Directionality of neuromodulation was further analyzed with radial cortical electric field plots (figures 3 and 5). The radial plots represented the inward and outward component of electric field normal to the cortical surface rather than just the vector magnitude. For cortical stimulation, it is theorized that electric field normal to the surface produced optimal polarization of cortical neurons projecting along cortical columns such as layer 5 pyramidal neurons (Jefferys *et al* 2003, Radman *et al* 2009, Rahman *et al* 2013).This ignores the potential contribution from tangential current flow, for example polarizing afferent axons (Bikson *et al* 2004, Rahman *et al* 2013). Modeling analysis takes account of this physiological assumption by projecting the local surface normal onto the local electric field ($n \cdot E$). Inward electric field can be interpreted as the effect due to anodal stimulation (excitatory), where as outward electric field represents cathodal (inhibitory) (Nitsche and Paulus 2000). However, the excitatory and inhibitory effects predicted are local to the neuron and distinct from more complex behavioral effects that may rely on a non-linear process and interactions across a network.

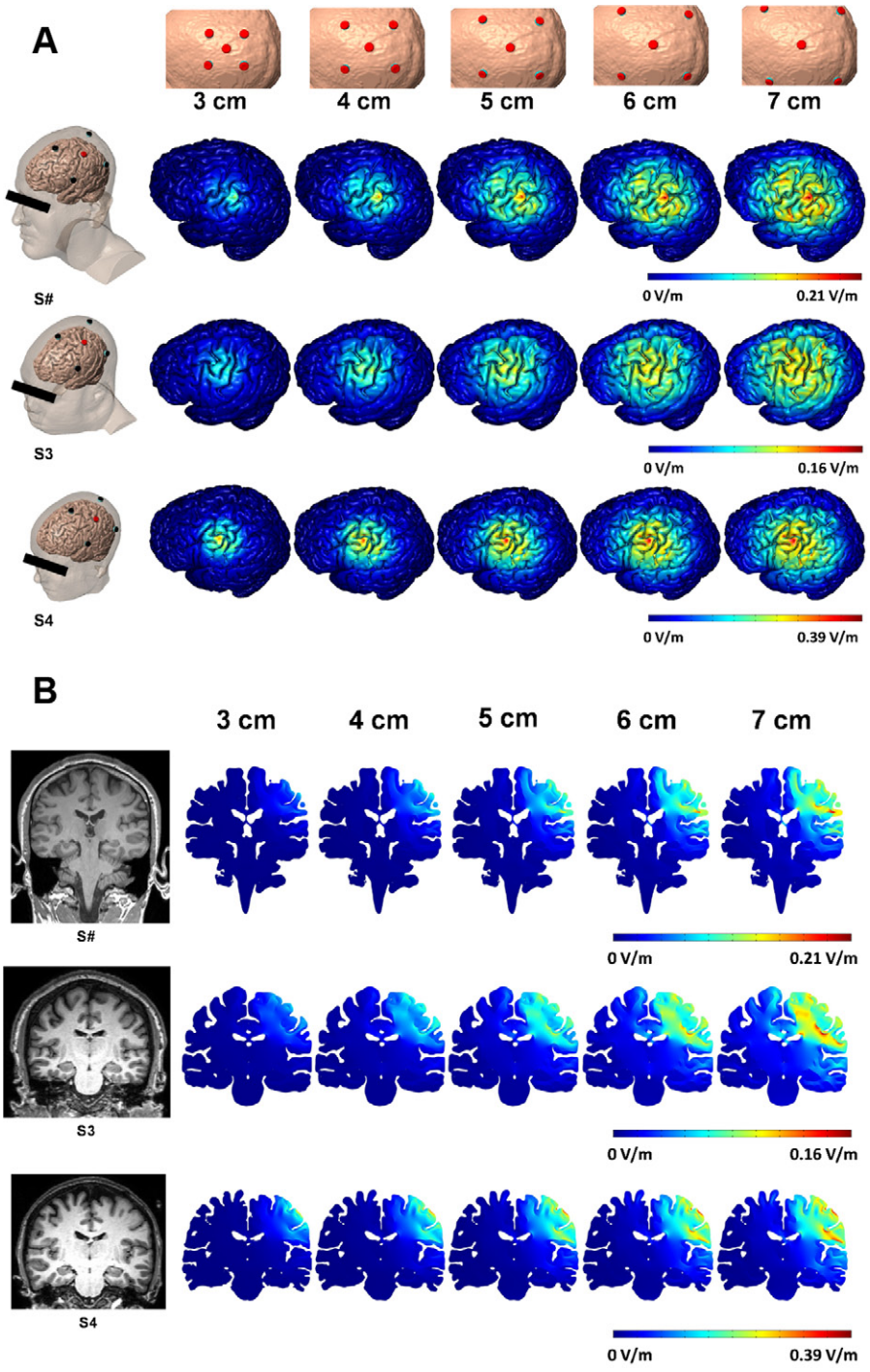

Figure 2. Finite Element Analysis of cortical electric field magnitude generated in three subjects during 4 × 1 HD-tDCS stimulation. The radius of the 4 × 1 ring was varied from 3 cm to 7 cm. Cortical E-field intensity increased with increasing ring radius, but a loss of spatial focality was observed.

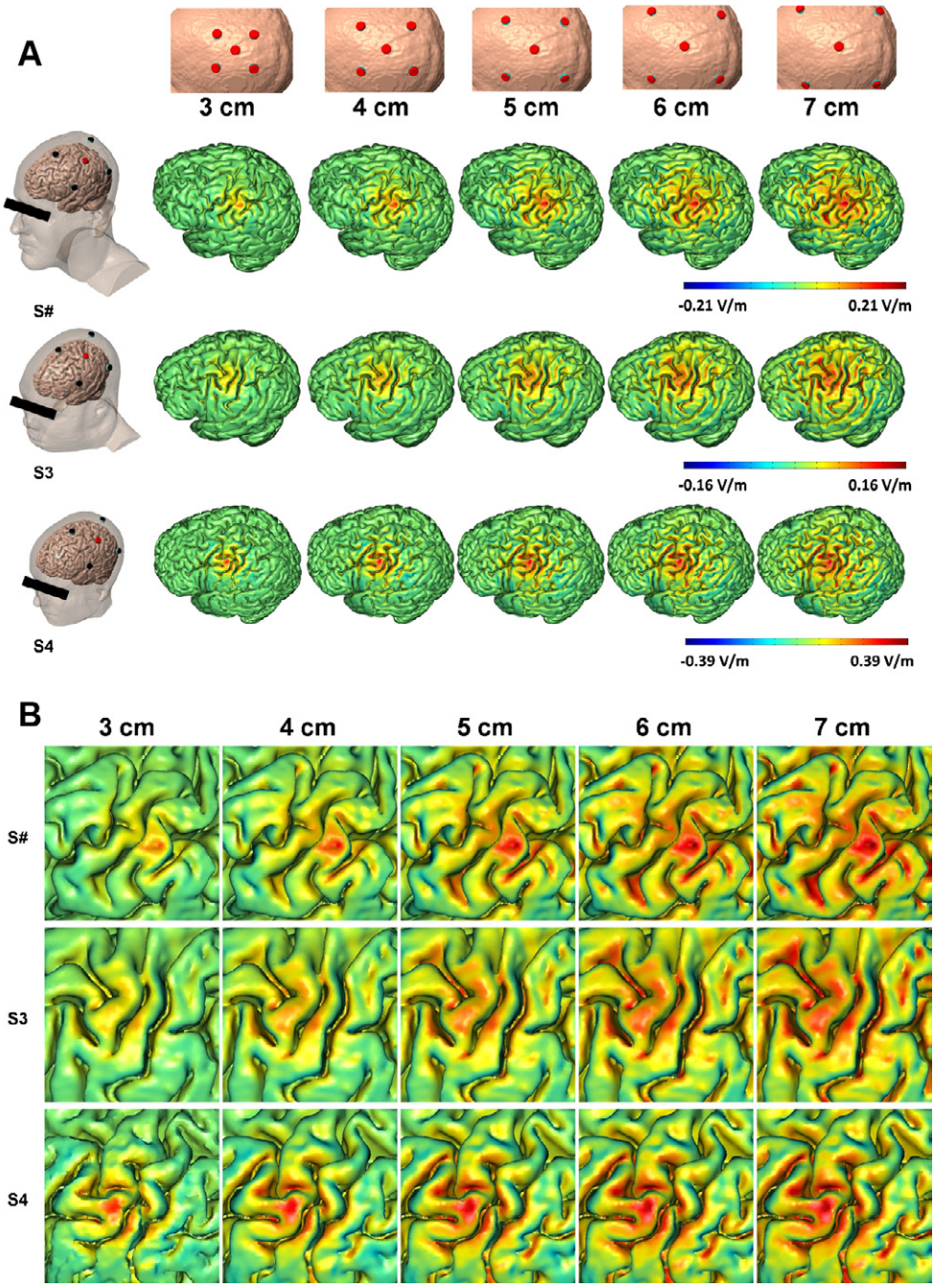

Figure 3. Radial Electric Field comparison. Anodal (red) and cathodal (blue) stimulation are compared as the normal component of electric field. Increasing ring radius from 3 cm to 7 cm had a similar intensity focality tradeoff as the overall electric field magnitude seen in figure 1. The peak intensity of both anodal and cathodal field increases with radius, but this increase is not proportional. Figure 6 further analyzes the relative anodal and cathodal peak intensities.

3.3. General role of surround electrode number

We simulated brain current flow produced with varied number of ring electrodes (eight models for S# with eight different cathode combinations with a center anode, figure 4). The electric field magnitude changed as the number of return electrodes increased from one to three; however, the electric field distribution was nearly identical from four to eight return electrodes. Thus, adding more than four cathodes may be redundant. Consideration of directionality resulted in similar findings and conclusions (figure 5). Five additional models were run on each of S3 and S4 (figure 4(B)). These models showed the same pattern—that 4 × 1 and onwards are redundant.

3.4. Quantified and inter-individual differences with radius

For any given head, the peak electric field increased approximately linearly with radius (figure 6(B)), but with significant variably across subjects. We further considered brain current flow skewness as ring radius was changed. This skewness value was derived from the perpendicular component of the electric field calculated in figures 3 and 5. A histogram of all the surface elements (from the directionality plot) with their respective normal electric field values was created. Skewness of this histogram was calculated as a measure of how far in the positive or negative direction the distribution tail extends. A more positive skewness value signified a greater proportion of anodal to cathodal peak intensities, while negative skewness represented the opposite. A skewness of zero would be a balanced. The skewness becomes less positive as the radius increases (figure 6(B)) indicating that the amount of peak anodal and peak cathodal stimulation becomes more balanced, though this value never reaches that of a one anode one cathode (1 × 1) configuration (figure 6(E)). Conventional 1 × 1 tDCS often assumes monopolar stimulation over an 'active' electrode, while in actuality the effects of both anode and cathode are still present. Concentric ring HD-tDCS does not eliminate stimulation of both polarities, but can skew the stimulation polarity in favor of the center electrode.

A third metric considered was a measure of the electric field distribution. The percentage of elements within 90% of the peak electric field was calculated for each model. This serves as a quantification of the cortical plots from figure 2(A). As expected, the electric filed distribution increased as the radius of the ring was increased (figure 6(C)).

3.5. Quantified and inter-individual differences with number of electrodes

The same metrics (peak electric field, skewness, and distribution) were considered in the analysis of effect of number of ring electrodes. This quantification confirmed that a 4 × 1 HD-tDCS montage has an effective number of return electrodes to use. Since increasing the number of return electrode above four produced no significant chance in brain current flow metrics, additional ring electrodes (beyond 4) were redundant.

The peak electric field 4 × 1 to 7 × 1 was effectively identical (figure 6(D)). Maximum predicted electric field with one cathode was higher, presumably due to less shunting, where the current shorts through more superficial head layers such as skin and CSF before reaching the brain. This value decreased drastically with two cathodes and diminished more with three cathodes. However, the peak electric field remains constant from four to seven cathodes, and slightly increased at eight.

Increasing the number of return electrodes (figure 6(E)) caused a more positive skew, though this effect saturated near four return electrodes. Montages utilizing a 1 × 1 configuration

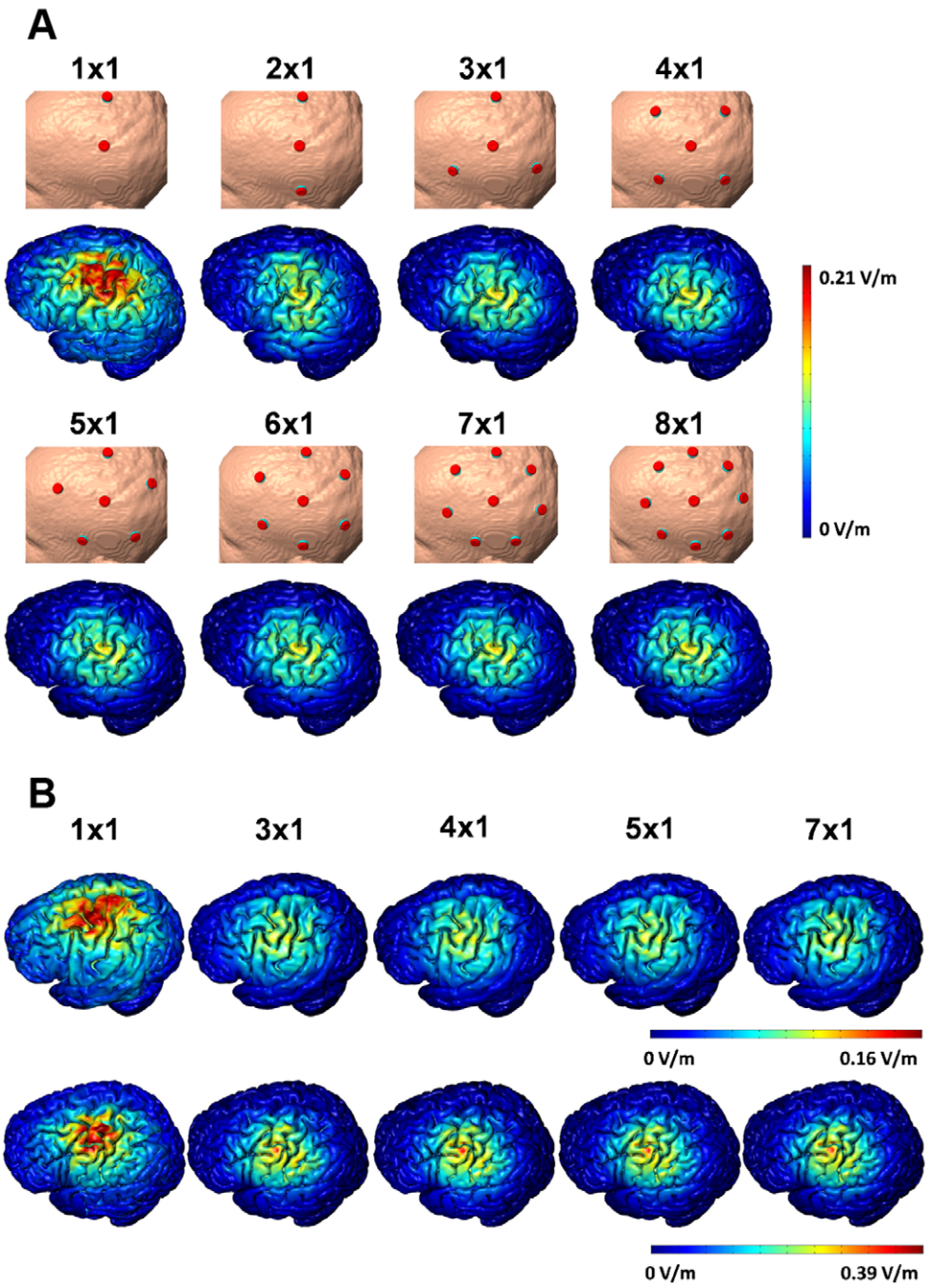

Figure 4. Finite Element Analysis of cortical electric field magnitude. The number of return electrodes (cathodes) were increased from one to eight. One, two, and three cathodes vary in terms of spatial distribution, while four and more cathodes are approximately the same.

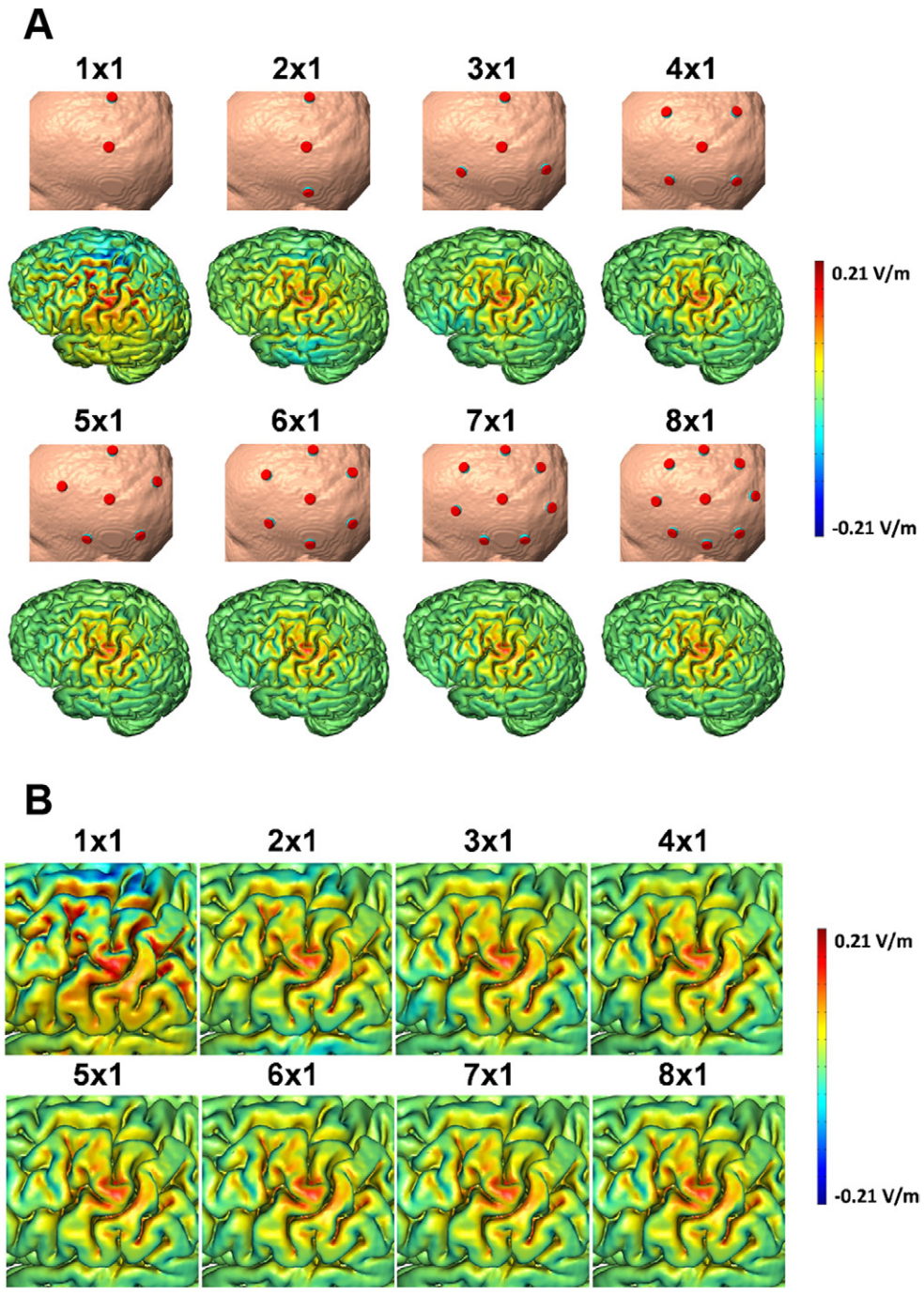

Figure 5. Finite Element Analysis of radial electric field with varying number of return electrodes (cathodes). Increasing the number of cathodes disperses and lowers the intensity of cathodal stimulation (blue) while the intensity of anodal stimulation remains relatively unchanged after two cathodes are introduced. Outward electric field peaks closely follow the position of the cathodes initially, but the effect becomes unnoticeable after four electrodes.

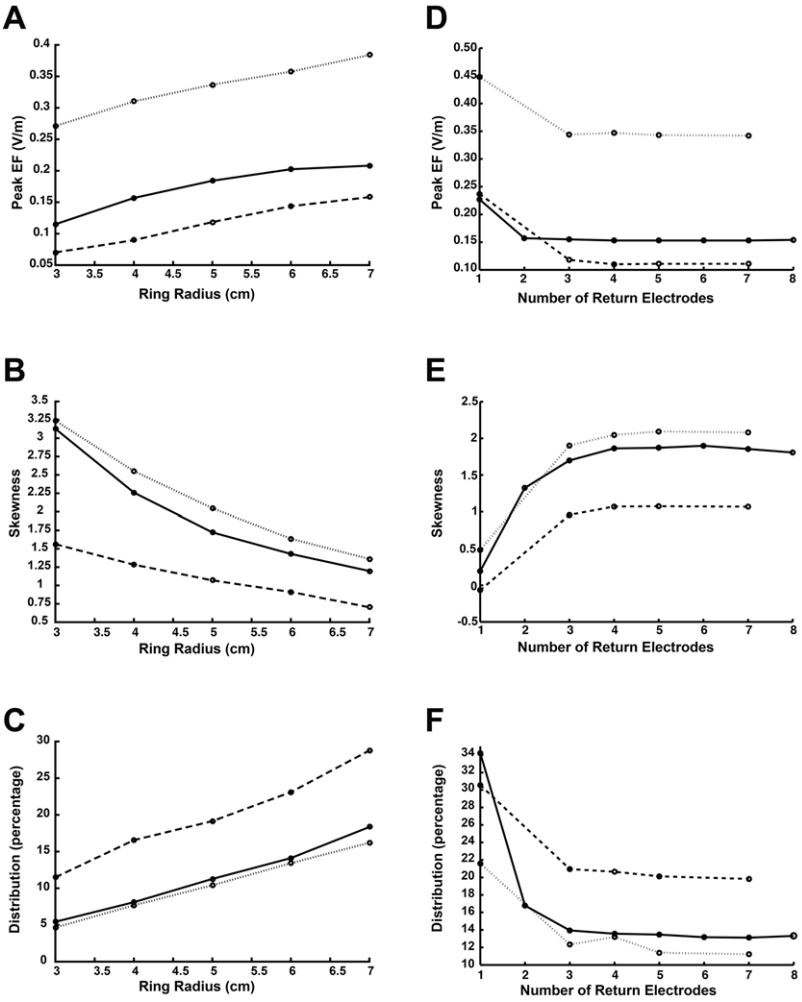

Figure 6. Quantification of results from figures 2, 3(A)–(C), 4 and 5(D)–(F). Ring radius was varied while keeping the number of return electrodes (4) constant in panels (A)–(C). The number of return electrodes was varied while keeping ring radius (5 cm) constant in panels (D)–(F). Electric Field is given in V/m for 1 mA of stimulation. Peak Cortical Electric field for three subjects (S4 dotted, S3 dashed, S# solid) was compared at 3, 4, 5, 6, and 7 cm HD montage radius (A). Despite individual differences within the same montage, all three subjects show increasing cortical electric field with increasing montage radius. Peak electric field decreases with additional return electrodes (D). Histograms of the component of electric field normal to the cortical surface (inward and outward field defined as positive and negative) were produced and the skewness of those distributions in the positive or negative direction calculated (B) and (E). Skewness of radial electric field distribution was compared between subjects while varying ring radius and number of return electrodes. The smallest radii configurations had the highest positive skewness indicating a greater proportion of anodal to cathodal peaks (B). Increasing radii resulted in a lowered positive skewness that nonetheless never reaches the skewness of 1×1 stimulation. Stimulation with one anode and one cathode (1×1) results in minimal skewness meaning almost equal amounts of peak anodal and cathodal stimulation. Additional return electrodes cause a greater imbalance in anodal to cathodal peak intensity resulting in more positive skewness (E). This corroborates the qualitative analysis in figure 3 which showed a dispersal of cathodal intensities. Spatial focality was quantified as the percentage of surface elements within 90% of peak electric field (F). Increasing ring radius predictably increases the spread of electric field. Increasing the number of return electrodes increases spread as well, but this spread saturates near four or more return electrodes.

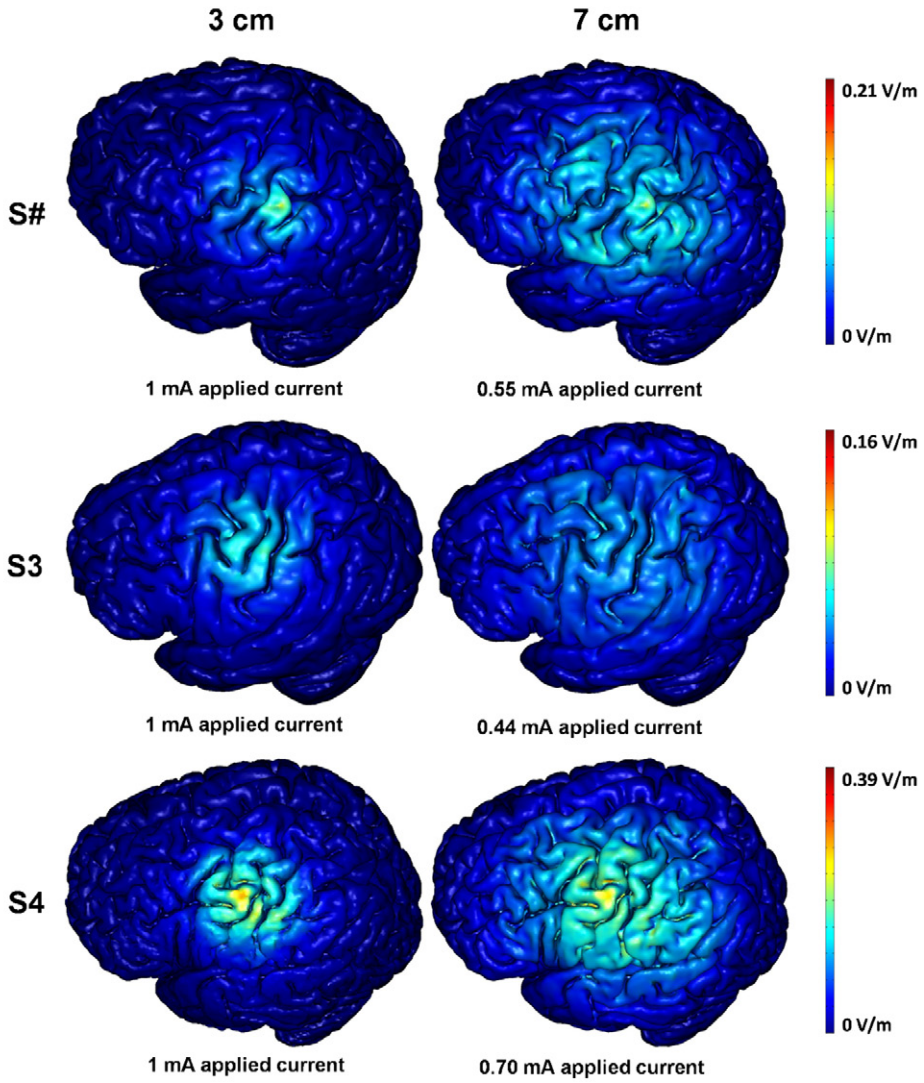

Figure 7. Due to the linearity of direct current physics, induced cortical electric field is predicted to scale with the applied current. The intensity tradeoff between a small radius (3 cm) and large radius (7 cm) 4 × 1 ring can be offset by scaling the applied stimulator current. Ring diameter is proposed as another method to adjust cortical electric field with possible utility in cases where applied current must be limited due to hardware or safety limitation. Other applications include the development of sham montages to blind subjects to stimulation.

were minimally skewed meaning there was nearly as much peak cathodal stimulation as peak anodal.

Lastly, the percentage of elements within 90% of the peak was even after 4 × 1 (figure 6(F)). The pattern seen here was similar to peak electric field because this measurement was based on the peak electric field in each model. Using this metric, however, it was predicted that the electric field distribution does not vary significantly after 3 × 1, and even more so after 4 × 1.

4. Discussion and conclusions

HD-tDCS includes any configuration using HD electrodes (Dmochowski 2011), which can be optimized for intensity or focality, or any other criterion. The concentric-ring configuration, with one center electrode surrounded by electrodes of the opposite polarity is thus just one HD embodiment. But, it is an embodiment that has been explored extensively, specifically using the 4 × 1 montage (Borckardt *et al* 2009, Datta *et al* 2009, Suh *et al* 2010, Caparelli-Daquer *et al* 2012, Edwards *et al* 2013, Brunyé *et al* 2014, Roy *et al* 2014, Heimrath *et al* 2015, Nikolin *et al* 2015, Shekhawat *et al* 2016, Zito *et al* 2015, Castillo-Saavedra *et al* 2016, Flood *et al* 2016, Kuo *et al* 2013). The simple reason is that it allows straightforward heuristic montage design, where the center electrode is placed over the target, the center polarity is selected based on a desire to excite (anode) or inhibit (cathode) the target, and the surrounded electrodes are set to define the area of cortex to be stimulated. The decision to use 4 electrodes in the surround, typically at distances of 5–7 cm, may derive largely from historical reasons and this design decision is addressed here in detail. Previous modeling studies have identified characteristics of concentric HD-tDCS such as focality and polarity specificity (Datta *et al* 2009, Villamar *et al* 2013b), but a systematic study has yet to be published.

This study aimed to assess the role of (1) ring radius and the (2) number of electrodes on the application of HD-tDCS with concentric montages using FEM modeling. Three high-resolution anatomically accurate head models were studied to consider inter-individual differences. We predicted that altering ring radius and the number of return electrodes (figures 2, 4 and 6) can affect cortical electric field intensity; though, there is a tradeoff between intensity and focality (figure 6), increasing focality being defined as the narrowing of the spatial distribution of cortical electric field relative to peak (figure 6(E)). It is suspected that at smaller radii a greater proportion of the total current shunts in a direct path through the relatively conductive skin. This loss of intensity in turn limits the spread of electric field and increases focality.

Besides affecting electric field magnitude, ring radius and return electrode number was found to modulate the relative concentrations of inward and outward electric field. Qualitatively, this is demonstrated in figures 3 and 5 as the relative imbalance of anodal (red) and cathodal (blue) intensity; the most obvious change being the increase from 1 surrounding cathode to 2 and then 3 (figure 5(B)). Due to the conservation of current, inward and outward current through an enclosed volume (i.e. the brain) is equal; however, the concentration of current in and out of the surface (normal current density, $n \cdot J$) may vary. This can lead to a balance between high intensity inward current density over a small area and low intensity outward current density over a large area. Electric field, being proportional to current density ($E = J/\sigma$), scales with current density and is subject to this behavior. Plotting a histogram of normal electric field from the cortical surface demonstrated the balance between inward and outward field as approximated by a Gaussian distribution centered at 0. However, this distribution can be asymmetric with peak inward and outward electric field (the tails of the distribution) shifting preferentially towards either side (figures 6(B) and (E)). At small radii, the increase in skewness may be a reflection on the overall increase in focality. In addition, it is important to consider that although there was individual variability across the three models, the patterns remained consistent. The results for the number of cathodes indicated that anything higher than 4 × 1 is unnecessary.

In general, the magnitude of the peak electric field increased as the distance between electrodes was increased. More of the brain was stimulated as well. The entire area underneath the ring formed by the electrodes was stimulated each time (figure 2). In addition, the stimulation would reach deeper down, into the white matter, as the radius was increased (figure 3).

The fact that focality decreased as ring radius was increased is contrary to the purpose of concentric HD-tDCS—to stimulate only a specific part of the brain. But on the other hand, the electric field decreased as well. This decrease in brain electric field can be compensated by increasing the amount of total current applied, though this affects tolerability and safe limits for skin irritation should not be exceeded (Minhas *et al* 2010).

Since increasing the radius increased the induced cortical electric field, this can be viewed as an alternative to increasing the applied stimulator current (figure 7). When there is a limit to how much current can be applied due to safety and comfort, ring radius can be modified instead to create a more intense electric field. Reducing ring radius would allow for the opposite; cortical electric field can be reduced while maintaining stimulator intensity. While the latter condition would be deleterious to neuromodulation, it creates another avenue for sham stimulation. Sham stimulation in tDCS is commonly applied as a relatively short (30 s) ramping of current at onset and offset with a period of no stimulation in between (Richardson *et al* 2014). However, at higher intensities subjects may feel stimulation throughout a session of tDCS. Reducing the induced cortical electric field while maintaining stimulator intensity could be a more effective sham protocol. Conversely, reducing the applied stimulator current while maintaining the induced cortical electric field could minimize sensation and further aid in subject blinding.

The appropriate ring radius to use ultimately depends on the intervention goals and practical considerations (e.g. unknowns about precise target location, limitations in set-up accuracy). In regards to number of electrodes, the 4×1 appeared as a preferred configuration since four surrounding electrodes are also sufficient to approximate a circle.

In comparison to conventional sponge pads, 4×1 HD-tDCS has a number of advantages; the most pronounced being focality. Studies with a mechanistic, anatomical, emphasis could be better served by this more precise method of stimulation that could avoid potentially confounding brain regions. Still, conventional pad stimulation has an extensive history of use. Clinicians may feel comfortable relying on the established safety record of conventional pads, but modeling results suggest much more spatial and polarity control utilizing the 4×1 configuration. This degree of control can be leveraged in cases where an additional safety factor would be warranted, particularly in susceptible populations (e.g. implants or skull defects). As more is understood about the brain and how different regions may affect clinical outcomes, 4×1 HD-tDCS can provide both the spatial and polarity precision needed to target these regions.

References

Alonzo A, Brassil J, Taylor J L, Martin D and Loo C K 2012 Daily transcranial direct current stimulation (tDCS) leads to greater increases in cortical excitability than second daily transcranial direct current stimulation *Brain Stimulat.* **5** 208–13

Antal A, Bikson M, Datta A, Lafon B, Dechent P, Parra L C and Paulus W 2014 Imaging artifacts induced by electrical stimulation during conventional fMRI of the brain *Neuroimage* **85** 1040–7

Antal A, Kincses T Z, Nitsche M A, Bartfai O and Paulus W 2004 Excitability changes induced in the human primary visual cortex by transcranial direct current stimulation: direct electrophysiological evidence *Invest. Ophthalmol. Vis. Sci.* **45** 702–7

Baker J M, Rorden C and Fridriksson J 2010 Using transcranial direct-current stimulation to treat stroke patients with aphasia *Stroke* **41** 1229–36

Bikson M, Dmochowski J and Rahman A 2013 The 'quasi-uniform' assumption in animal and computational models of non-invasive electrical stimulation *Brain Stimulat.* **6** 704–5

Bikson M, Inoue M, Akiyama H, Deans J K, Fox J E, Miyakawa H and Jefferys J G R 2004 Effects of uniform extracellular DC electric fields on excitability in rat hippocampal slices *in vitro J. Physiol.* **557** 175–90

Bikson M, Truong D Q, Mourdoukoutas A P, Aboseria M, Khadka N, Adair D and Rahman A 2015 Modeling sequence and quasi-uniform assumption in computational neurostimulation *Prog. Brain Res.* **222** 1–23

Borckardt J J, Smith A R, Reeves S T, Madan A, Shelley N, Branham R, Nahas Z and George M S 2009 A pilot study investigating the effects of fast left prefrontal rTMS on chronic neuropathic pain *Pain Med.* **10** 840–9

Brunyé T T, Cantelon J, Holmes A, Taylor H A and Mahoney C R 2014 Mitigating cutaneous sensation differences during tDCS: comparing sham versus low intensity control conditions *Brain Stimulat.* **7** 832–5

Caparelli-Daquer E M, Zimmermann T J, Mooshagian E, Parra L C, Rice J K, Datta A, Bikson M and Wassermann E M 2012 A pilot study on effects of 4 × 1 high-definition tDCS on motor cortex excitability *Annual Int. Conf. of the IEEE Engineering in Medicine and Biology Society* pp 735–8

Castillo-Saavedra L *et al* 2016 Clinically effective treatment of fibromyalgia pain with high-definition transcranial direct current stimulation: phase II open-label dose optimization *J. Pain* (*Off. J. Am. Pain Soc.*) **17** 14–26

Datta A, Bansal V, Diaz J, Patel J, Reato D and Bikson M 2009 Gyri-precise head model of transcranial direct current stimulation: improved spatial focality using a ring electrode versus conventional rectangular pad *Brain Stimulat.* **2** 201–7, 207.e1

Datta A, Truong D, Minhas P, Parra L C and Bikson M 2012 Inter-individual variation during transcranial direct current stimulation and normalization of dose using MRI-derived computational models *Front. Psychiatry* (*Front. Res. Found.*) **3** 91

Datta A, Zhou X, Su Y, Parra L C and Bikson M 2013 Validation of finite element model of transcranial electrical stimulation using scalp potentials: implications for clinical dose *J. Neural Eng.* **10** 036018

Dmochowski J P, Datta A, Bikson M, Su Y and Parra L C 2011 Optimized multi-electrode stimulation increases focality and intensity at target *J. Neural Eng.* **8** 046011

Dmochowski J P, Datta A, Huang Y, Richardson J D, Bikson M, Fridriksson J and Parra L C 2013 Targeted transcranial direct current stimulation for rehabilitation after stroke *Neuroimage* **75** 12–9

Donnell A, Nascimento T D, Lawrence M, Gupta V, Zieba T, Truong D Q, Bikson M, Datta A, Bellile E and DaSilva A F 2015 High-definition and non-invasive brain modulation of pain and motor dysfunction in chronic TMD *Brain Stimulat.* **8** 1085–92

Edwards D, Cortes M, Datta A, Minhas P, Wassermann E M and Bikson M 2013 Physiological and modeling evidence for focal transcranial electrical brain stimulation in humans: a basis for high-definition tDCS *Neuroimage* **74** 266–75

Flood A, Waddington G and Cathcart S 2016 High-definition transcranial direct current stimulation enhances conditioned pain modulation in healthy volunteers: a randomized trial *J. Pain* **17** 600–5

Fregni F *et al* 2005 Anodal transcranial direct current stimulation of prefrontal cortex enhances working memory *Exp. Brain Res.* **166** 23–30

Fregni F *et al* 2006 A sham-controlled, phase II trial of transcranial direct current stimulation for the treatment of central pain in traumatic spinal cord injury *Pain* **122** 197–209

Heimrath K, Breitling C, Krauel K, Heinze H-J and Zaehle T 2015 Modulation of pre-attentive spectro-temporal feature processing in the human auditory system by HD-tDCS *Eur. J. Neurosci.* **41** 1580–6

Huang Y, Dmochowski J P, Su Y, Datta A, Rorden C and Parra L C 2013 Automated MRI segmentation for individualized modeling of current flow in the human head *J. Neural Eng.* **10** 066004

Hummel F, Celnik P, Giraux P, Floel A, Wu W H, Gerloff C and Cohen L G 2005 Effects of non-invasive cortical stimulation on skilled motor function in chronic stroke *Brain* **128** 490–9

Jefferys J G, Deans J, Bikson M and Fox J 2003 Effects of weak electric fields on the activity of neurons and neuronal networks *Radiat. Prot. Dosim.* **106** 321–3

Kempe R, Huang Y and Parra L C 2014 Simulating pad-electrodes with high-definition arrays in transcranial electric stimulation *J. Neural Eng.* **11** 026003

Kuo H-I, Bikson M, Datta A, Minhas P, Paulus W, Kuo M-F, Nitsche M A 2013 Comparing cortical plasticity induced by conventional and high-definition 4 × 1 ring tDCS: a neurophysiological study *Brain Stimulat.* **6** 644–48

Minhas P, Bansal V, Patel J, Ho J S, Diaz J, Datta A and Bikson M 2010 Electrodes for high-definition transcutaneous DC stimulation for applications in drug delivery and electrotherapy, including tDCS *J. Neurosci. Methods* **190** 188–97

Minhas P, Bikson M, Woods A J, Rosen A R and Kessler S K 2012 Transcranial direct current stimulation in pediatric brain: a computational modeling study *2012 Annual Int. Conf. of the IEEE Engineering in Medicine and Biology Society (EMBC) Presented at the 2012 Annual Int. Conf. of the IEEE Engineering in Medicine and Biology Society (EMBC)* pp 859–62

Miranda P C, Mekonnen A, Salvador R and Ruffini G 2013 The electric field in the cortex during transcranial current stimulation *Neuroimage* **70** 48–58

Nikolin S, Loo C K, Bai S, Dokos S and Martin D M 2015 Focalised stimulation using high definition transcranial direct current stimulation (HD-tDCS) to investigate declarative verbal learning and memory functioning *Neuroimage* **117** 11–9

Nitsche M A and Paulus W 2000 Excitability changes induced in the human motor cortex by weak transcranial direct current stimulation *J. Physiol.* **527** 633–9

Peterchev A V, Wagner T A, Miranda P C, Nitsche M A, Paulus W, Lisanby S H, Pascual-Leone A and Bikson M 2012 Fundamentals of transcranial electric and magnetic stimulation dose: definition, selection, and reporting practices *Brain Stimulat.* **5** 435–53

Radman T, Ramos R L, Brumberg J C and Bikson M 2009 Role of cortical cell type and morphology in subthreshold and suprathreshold uniform electric field stimulation *in vitro Brain Stimul.* **2** 215–28

Rahman A, Reato D, Arlotti M, Gasca F, Datta A, Parra L C and Bikson M 2013 Cellular effects of acute direct current stimulation: somatic and synaptic terminal effects *J. Physiol.* **591** 2563–78

Richardson J D, Fillmore P, Datta A, Truong D, Bikson M and Fridriksson J 2014 Toward development of sham protocols for high-definition transcranial direct current stimulation (HD-tDCS) *Neuroregulation* **1** 62

Roy A, Baxter B and He B 2014 High-definition transcranial direct current stimulation induces both acute and persistent changes in broadband cortical synchronization: a simultaneous tDCS-EEG study *IEEE Trans. Biomed. Eng.* **61** 1967–78

Shekhawat G S, Sundram F, Bikson M, Truong D, De Ridder D, Stinear C M, Welch D and Searchfield G D 2016 Intensity, duration, and location of high-definition transcranial direct current stimulation for tinnitus relief *Neurorehabil. Neural Repair.* **30** 349–59

Suh H S, Kim S-H, Lee W H and Kim T-S 2009 Realistic simulation of transcranial direct current stimulation via 3D high-resolution finite element analysis: effect of tissue anisotropy *Annual Int. Conf. of the IEEE Engineering in Medicine and Biology Society, 2009* pp 638–41

Suh H S, Lee W H, Cho Y-S, Kim J-H and Kim T-S 2010 Reduced spatial focality of electrical field in tDCS with ring electrodes due to tissue anisotropy *2010 Annual Int. Conf. of the IEEE Engineering in Medicine and Biology* pp 2053–6

Truong D Q, Magerowski G, Blackburn G L, Bikson M and Alonso-Alonso M 2013 Computational modeling of transcranial direct current stimulation (tDCS) in obesity: impact of head fat and dose guidelines *Neuroimage Clin.* **2** 759–66

Villamar M F, Volz M S, Bikson M, Datta A, Da Silva A F and Fregni F 2013a Technique and considerations in the use of 4×1 ring high-definition transcranial direct current stimulation (HD-tDCS) *J. Vis. Exp.* **77** e50309

Villamar M F, Wivatvongvana P, Patumanond J, Bikson M, Truong D Q, Datta A and Fregni F 2013b Focal modulation of the primary motor cortex in fibromyalgia using 4×1-ring high-definition transcranial direct current stimulation (HD-tDCS): immediate and delayed analgesic effects of cathodal and anodal stimulation *J. Pain* **14** 371–83

Wagner T, Fregni F, Fecteau S, Grodzinsky A, Zahn M and Pascual-Leone A 2007 Transcranial direct current stimulation: a computer-based human model study *NeuroImage* **35** 1113–24

Wagner S, Rampersad S M, Aydin Ü, Vorwerk J, Oostendorp T F, Neuling T, Herrmann C S, Stegeman D F and Wolters C H 2014 Investigation of tDCS volume conduction effects in a highly realistic head model *J. Neural Eng.* **11** 016002

Xu J, Healy S M, Truong D Q, Datta A, Bikson M and Potenza M N 2015 A feasibility study of bilateral anodal stimulation of the prefrontal cortex using high-definition electrodes in healthy participants *Yale J. Biol. Med.* **88** 219–25 (PMCID: PMC4553641)

Zito G A, Senti T, Cazzoli D, Müri R M, Mosimann U P, Nyffeler T and Nef T 2015 Cathodal HD-tDCS on the right V5 improves motion perception in humans *Front. Behav. Neurosci.* **9** 257